FULL PAPER

Variation of the optical properties with size and composition of small, isolated Cd$_x$Se$_y^+$ clusters

Marc Jäger [ORCID] | Rolf Schäfer

Technische Universität Darmstadt, Eduard-Zintl Institut für Anorganische und Physikalische Chemie, Darmstadt, Germany

Correspondence
Marc Jäger, Technische Universität Darmstadt, Eduard-Zintl Institut für Anorganische und Physikalische Chemie, Alarich-Weiss-Straße 8, 64287 Darmstadt, Germany.
Email: jaeger@cluster.pc.chemie.tu-darmstadt.de

Funding information
Deutsche Forschungsgemeinschaft, Grant/Award Number: SCHA 885/15-2

Abstract

Global energy minimum structures and optoelectronic properties are presented for isolated Cd$_x$Se$_y^+$ clusters with $x + y \leq 26$. The compositional- and size-dependent variation of optical, electronic and geometric properties is systematically studied within the framework of ground state and time-dependent density functional theory. The applied methods are justified by benchmarks with experimental data. It is shown that the optical gap can be tuned by more than 2 eV by only changing the composition for a fixed number of atoms. The stoichiometric species reveal an unexpected size-dependent behavior in comparison to larger colloidal CdSe quantum dots, that is, a redshift of the optical gap was observed with decreasing cluster size in contrast to predictions by quantum-size effects. This unexpected result is discussed in detail taking the positive charge of the clusters into account.

KEYWORDS

CdSe, cluster, density functional theory, DFT, genetic algorithm, global optimization, nanoparticle, optical absorption, optical gap, optoelectronic properties, quantum dot, semiconductor

1 | INTRODUCTION

A fundamental understanding of how exactly physicochemical properties evolves with particle size and composition is one of the central issues in the research of new materials. The driving force to investigate clusters is the endeavor to close the knowledge gap and to understand how material properties develop with respect to various parameters such as particle size and composition. In addition, this can also lead to new insights for a rational material design. In the present work, it is systematically shown how optoelectronic properties and geometries of the smallest isolated Cd$_x$Se$_y^+$ clusters develop with system size and composition. Surprisingly, their optical behavior is almost opposite to CdSe quantum dots (QDs).

Semiconductor nanoparticles (NPs), especially CdSe QDs have drawn large attention due to their intriguing optical properties, which leads to a variety of applications such as light emitting diodes (LEDs), displays, biomedical imaging and lasers.[1–5]

In the past CdSe NPs and clusters have been examined in theoretical and experimental investigations.[6–19] Most theoretical studies deal with isolated stoichiometric neutral CdSe clusters.[15–19] Overall, there are only few studies on charged CdSe clusters and non-stoichiometric CdSe clusters.[6–8] But, there are no studies that examine all possible compositions up to a certain particle size and its effects on geometrical and optoelectronic properties in detail. However, in order to gain a better understanding of the evolution of optoelectronic properties, it is necessary to systematically investigate isolated species depending on their size and chemical composition. Since we investigated a few selected cationic CdSe clusters in previous combined experimental and theoretical studies[6,7] and there is overall less work on cationic CdSe clusters than on neutral ones, this

work presents a full examination of small cationic $Cd_xSe_y^+$ clusters with $x + y \leq 26$. All stoichiometries from pure Cd_x^+ to pure Se_y^+ clusters are studied up to 8 atoms and because of the exponentially increasing computational efforts of the global optimization calculations, only stoichiometric species are considered for larger clusters. The paper is organized as the following: First the methodology is explained and then geometrical and optoelectronical trends are considered and analyzed. When discussing the results, first, the limiting cases of pure Cd_x^+ and pure Se_y^+ clusters are taken into account and then the influence of the composition is analyzed explicitly.

2 | METHODOLOGY

Lowest energy structures of $Cd_xSe_y^+$ clusters are obtained via unbiased global optimization (GO) by employing our genetic algorithm (GA)[20] as described elsewhere.[6,7] All energetically lowest-lying isomers are locally reoptimized using NWChem v6.6[21] at the PBE0/cc-pVTZ-PP[22–24] and B3LYP/cc-pVTZ-PP[24–26] level of theory with the corresponding effective core potentials, since in a benchmark as well as in latest joined experimental and theoretical studies both xc functional/basis set combinations have pointed out to provide a very good description for $Cd_xSe_y^+$ clusters.[6,7] The results of the benchmark calculations are shown in Figure S1 and Figure S2 of the supporting information. A doublet state as electronic spin multiplicity was obtained for all of the lowest energy species. Harmonic frequency analysis is performed for all isomers at the particular level of theory in order to verify that the optimized geometries correspond to local minima on the potential energy surface. For the putative global minimum (GM), that is, the lowest energy structure of each cluster composition

regarding both level of theories, electronic excitation spectra are calculated using spin-unrestricted time-dependent density functional theory (TDDFT), employing the same xc functionals and basis sets as used during the geometry optimization. Due to the huge computational effort, in case of the larger clusters with $x + y \geq 20$ the smaller basis set cc-pVDZ-PP was employed in the TDDFT calculations.

3 | RESULTS AND DISCUSSION

3.1 | Geometries

In Figure 1 and in Figure 2 the putative GM for the $Cd_xSe_y^+$ species with $x + y \leq 8$ and the stoichiometric clusters up to 26 atoms are depicted, respectively. Species with different lowest energy structures regarding both applied level of theories are highlighted by a red star. For those clusters, both lowest energy structures are shown in Figure S3 of the supporting information.

The first question is how does the stoichiometry affects the cluster geometry? This can be answered by considering the extreme cases with regard to the composition, i. e. analyzing the geometric structure of the pure Cd_x^+ and Se_y^+ clusters. On the one hand, it is noticeable that in the case of Cd_x^+ linear chain structures are formed up to $x = 5$. From $x = 5$ to $x = 6$ a 1d → 3d structural transition takes place. However, also in case of the 3d structures an elongated character is maintained. From $x = 6$ to $x = 8$ the number of four-fold coordinated Cd atoms increases from one to three. All these structures exhibit a trigonal bipyramidal Cd_5 unit as main building block. Previously, lowest-energy structures of Cd_x^+ clusters were reported.[27] In our GO procedure we have found all the proposed Cd_x^+ structures and
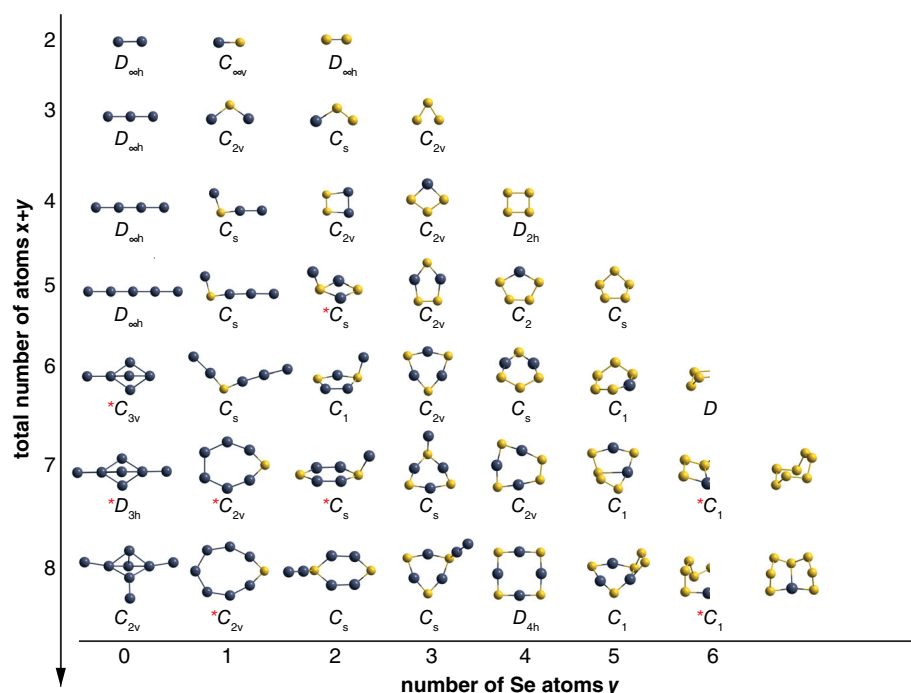
FIGURE 1 Lowest energy $Cd_xSe_y^+$ geometries with $x + y \leq 8$ (Cd: Dark atoms, Se: Light atoms) obtained by GO and a subsequent geometry refinement at the PBE0/cc-pVTZ-PP limiting are shown together with their point group symmetries. At each row the lowest energy structure for each composition (with $x + y$ = constant) is shown. Species whose lowest energy structure obtained by B3LYP/cc-PVTZ-PP differ from the one shown here are marked by a red star.
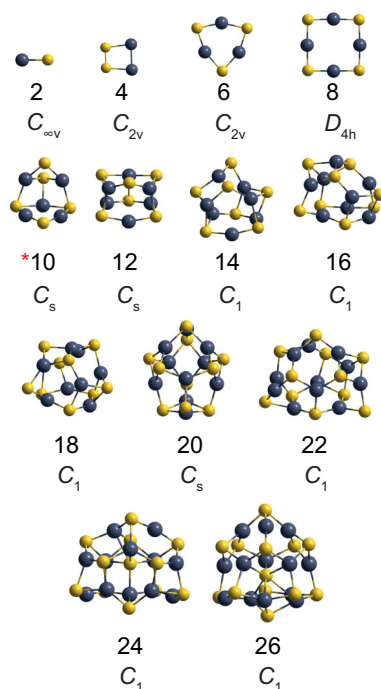
FIGURE 2 Lowest energy geometries for stoichiometric $Cd_xSe_y^+$ clusters with $10 \leq x + y \leq 26$ (Cd: Dark atoms, Se: Light atoms) obtained by GO and a subsequent geometry refinement at the PBE0/cc-pVTZ-PP level of theory are shown together with their point group symmetries. For each cluster the overall number of atoms ($x + y$) is given. Species whose lowest energy structure obtained by B3LYP/cc-PVTZ-PP differ from the one shown here are marked with a red star.

additionally new ones with lower energy for x = 4, 5, 7, 8. The energetic stabilization of the new lowest energy structures are given in eV in brackets relative to the ones recently proposed:[27] Cd_4^+ (0.14), Cd_5^+ (0.17), Cd_7^+ (0.14) and Cd_8^+ (0.02). On the other hand, pure Se_y^+ clusters for y = 3 already possess an angled geometry and larger species form ring structures as it is known for neutral Se clusters in which all selenium atoms are twofold coordinated.[28,29] The 2d → 3d transition takes place from y = 4 to y = 5.

Interestingly all stoichiometric and singly Se-doped species up to 8 atoms are planar. All clusters except $Cd_2Se_2^+$ have in common that the number of heteronuclear bonds is maximized by alternation of Cd and Se atoms. The exception of $Cd_2Se_2^+$ is due to the extraordinary stability of the Se_2 unit formed in this cluster which was already examined in detail.[6,7,30] An increase of the number of Se atoms leads to ring-like structures. The effect of the stoichiometry on the geometry can be seen particular well in the case of the pentamers: Starting with linear Cd_5^+ clusters, the replacement of one Cd (i.e., the formation of Cd_4Se^+) leads to angled 2-dimensional structure, whereas ring-like structures start at $Cd_3Se_2^+$. Especially when comparing $Cd_3Se_2^+$ with $Cd_2Se_3^+$ it can be seen that both clusters exhibit a planar ring. For $Cd_3Se_2^+$ an alternating four-membered CdSe ring is formed with an excess of Cd attached to a Se ring-atom, while in case of $Cd_2Se_3^+$

the additional Se atom is integrated in the ring by building a planar five-membered ring with a homonuclear Se—Se bond as it is known for instance for pure Se_y^+ clusters. A further substitution of Cd with Se breaks the planarity of the five-membered ring with three homonuclear Se—Se bonds. Obviously, the composition has a very large influence on the structure. Hence, two opposite trends are observed. On the one hand, a high proportion of Cd leads to a higher probability of forming planar structures as seen for Cd_xSe^+ species, while more Se leads to rings with Se—Se "zig-zag"-chains as observed in pure Se_y^+ clusters. For clusters up to eight atoms, in some cases, the $Cd_3Se_3^+$ structural motif seems to be particularly preferred since it is found in several species: $Cd_4Se_3^+$, $Cd_5Se_3^+$ and $Cd_3Se_5^+$.

Similar to larger neutral stoichiometric CdSe cluster, cationic CdSe cluster are made up of four-membered and six-membered rings as depicted in Figure 2. All stoichiometric $Cd_xSe_y^+$ clusters with at least 10 atoms are three dimensional. Hence, the 2d → 3d transition takes place from $Cd_4Se_4^+$ to $Cd_5Se_5^+$. The geometries exhibit a maximization of heteronuclear bonds with twofold and threefold coordinated atoms. The first endohedral cage structure is formed for 24 atoms, with one Se atom in the center which is coordinated by five Cd atoms. This is remarkable since the GM of the neutral counterpart is a hollow cubic structure and only for $Cd_{13}Se_{13}$ the first geometry with an endohedral atom occurs.[31] In the GO of $Cd_{12}Se_{12}^+$, the hollow cubic structure was also obtained but due to its positive charge it is distorted to a structure with C_s-symmetry which was also found by Sanville et al..[8] Although the energy of the hollow structure is lowered by lowering its symmetry, the energy difference to our found GM is still 0.10 eV for both levels of theory. For $Cd_{13}Se_{13}^+$ the central Se atom is coordinated by six Cd atoms.

In previous studies, a detailed analysis of the nature of the chemical bonding and the overall electronic structure of small, cationic, stoichiometric $(CdSe)_n^+$ clusters with n = 2–6 was already performed, so that it is waived here.[6,7]

3.2 | Optical properties

In this section, the variation of the optical properties of $Cd_xSe_y^+$ clusters is investigated with respect to the total number of atoms and the chemical composition. All optical absorption spectra are shown in the supporting information in Figure S4 and Figure S5. The comparison between PBE0 and B3LYP calculations exhibits, that the predicted spectra show a similar width and shape of absorption peaks but in most cases B3LYP spectra are more red-shifted.

In case of pure Cd_x^+ clusters, the 1d → 3d transition from Cd_5^+ to Cd_6^+ is heavily pronounced in the optical absorption. The absorption spectra from Cd_2^+ up to Cd_5^+ show a strong peak, which can be explained qualitatively by a particle in the box model. With more Cd atoms in the linear chain, this peak is shifted to smaller transition energies and becomes more intense. The absorption spectrum of the non-linear Cd_6^+ cluster becomes more complex, since there are many absorption signals that overlap. Contrary to the intense Cd_x^+ spectra,

pure Se_y^+ clusters exhibit a much weaker optical absorption. The absorption features of Se_y^+ increases with y, because the larger the cluster the more electronic transitions are found in the examined energy range and this leads to a stronger overlap of the absorption features. A general trend is visible for $Cd_xSe_y^+$ clusters: a higher amount of Cd shifts the optical absorption spectrum to higher transition energies. Each absorption signature is characteristic for the individual cluster composition and therefore, it serves as a finger print for the specific species. In case of the stoichiometric clusters (see Figure S5), the absorption spectra up to $Cd_4Se_4^+$ consist of well separated signals. It is striking that the spectra for species with $16 \leq x + y \leq 20$ are very similar to one another. The optical absorption begins with a weak signal from about 1 eV and proceeds with low intensity up to at least 2 eV. Starting from 3 eV, the intensity strongly increases and a first more intense absorption signal appears. This is followed by a characteristic dominant sharp peak around 4 eV and then the absorption intensity increases further for higher excitation energies. The structural transition to the cage structures is also reflected in the spectra, since both clusters, $Cd_{12}Se_{12}^+$ and $Cd_{13}Se_{13}^+$, already show around 2.3 eV an absorption feature with higher intensity than the others. Overall, the similarity between the absorption spectra of stoichiometric clusters with different sizes could be explained due to their structural similarities since all stoichiometric clusters only form heteronuclear bonds and all are built up of four-membered and six-membered rings connected to each other to build up 3d structures. For $Cd_8Se_8^+$ to $Cd_{13}Se_{13}^+$, especially noticeable is the size-independent position of the dominant absorption peak around 4 eV.
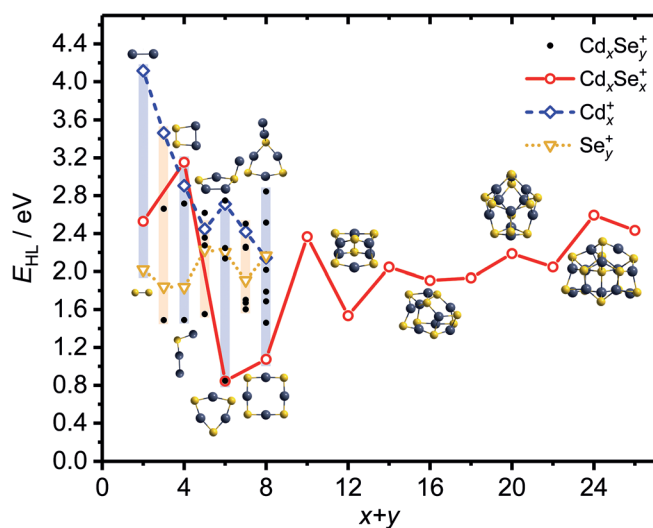

FIGURE 3 Size- and compositional-dependent HOMO-LUMO gaps E_{HL} calculated at the PBE0 level of theory for the $Cd_xSe_y^+$ global minimum structures with $x + y \leq 26$. The compositional effect for a constant number of atoms is highlighted by orange and blue bars. The connected red points show the property evolution of the stoichiometric ($x = y$) clusters. The connected blue diamonds show the variation of E_{HL} of Cd_x^+ species, whereas the yellow connected triangles represent the alteration of Se_y^+ clusters. The values of all remaining $Cd_xSe_y^+$ clusters are marked by a black point.

When studying optoelectronic properties of clusters, often used quantities are the HOMO-LUMO gap E_{HL}, the first electronic excitation energy $E_{g,1}$ and the optical gap E_g which is defined here as the first electronic excitation energy with an oscillator strength of $f_i \geq 0.001$. An important question is how those quantities evolve with particle size and composition? Hence, all aforementioned quantities are calculated and listed in Table S1 of the supporting information. When visualizing all quantities as function of the size $x + y$, it is striking that their course is very similar. For this reason, only E_{HL} is depicted in Figure 3 as an example. Here, for $x + y$ = constant the E_{HL} values of all possible compositions are shown. The range of this compositional dependency is marked by vertically aligned blue and orange bars. Additionally, for species with an even number of atoms the cluster structure of the highest and lowest E_{HL} value is shown. Black points represent non-stoichiometric $Cd_xSe_y^+$ clusters, red open circles indicate the stoichiometric clusters. The blue diamonds and the yellow down-facing triangles show the compositional limiting cases of pure Cd_x^+ and Se_y^+ clusters, respectively.

The value of E_{HL} of Cd_x^+ clusters generally decreases with increasing number of atoms (as expected from a simple particle in a box model). From five to six atoms, where the 1d → 3d transition takes place, there is a small discontinuity in the course. For a fixed size ($x + y$ = constant), Cd_x^+ clusters usually exhibit the upper limit of E_{HL}. Except for $x + y = 8$, here E_{HL} of Cd_8^+ is in the middle of the accessible range. In contrast, E_{HL} of pure Se_y^+ clusters mostly exhibits the smallest value, but shows overall a small increase up to $x + y = 8$. In case of the octamers E_{HL} of Se_8^+ is very close to the value of Cd_8^+ and therefore, in the middle of the range.

The compositional effect on the optoelectronic properties is clearly visible and highlighted by the range of the blue and orange bars. Accordingly, optoelectronic properties strongly dependent on the composition. For a fixed number of atoms, only the variation of the composition may cause a change in the optoelectronic property of more than 2 eV. Overall, the analysis shows that cluster size and chemical composition have a strong influence on the optical behavior of the system. With exception of $x + y = 4$, Cd-rich species exhibit large gaps. Interestingly, in case of the hexamers and octamers, the stoichiometric clusters ($Cd_3Se_3^+$ and $Cd_4Se_4^+$) show the smallest E_{HL} value of all possible compositions. In the case of $Cd_3Se_3^+$, this is due to the Jahn-Teller effect induced by the positive charge, which leads to a small splitting of the originally degenerate HOMOs of the neutral Cd_3Se_3.[7] The size-dependent variation of E_{HL} of stoichiometric clusters is decreasing from $Cd_2Se_2^+$ to $Cd_3Se_3^+$ and then for larger species an oscillating but also slightly increasing behavior is observed. The latter is astonishing since the optical gap for CdSe QDs behaves in exactly the opposite way and thus, increases with cluster size. The main reasons for the different observations are, besides the size range, the state of the charge and the chemical environment. These influences have already been intensively examined in previous studies.[6,7]

Experimental studies on colloidal CdSe NPs with different Cd/Se ratios have shown that an increasing amount of Cd leads also to an increase in the intensity of the optical absorption.[32] This raises the
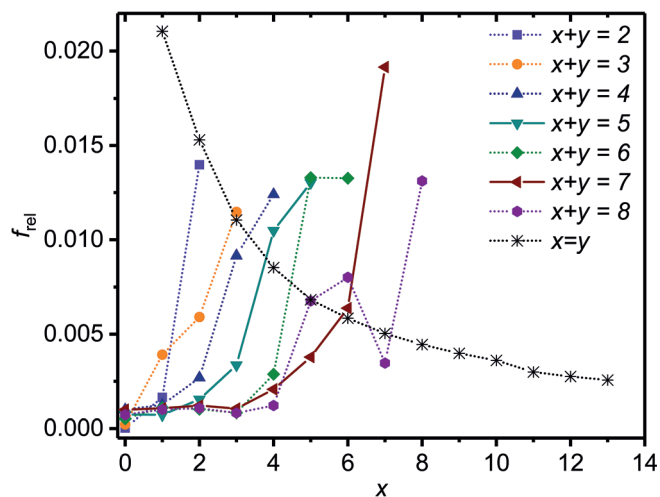
FIGURE 4 Dependency of the overall transition intensity, calculated by the sum of the oscillator strengths which is normalized to the total number of electrons f_{rel} up to 5.0 eV as function of the number of Cd atoms x within the cluster for all $Cd_xSe_y^+$ species.

FIGURE 5 Dependency of the HOMO-LUMO gap $E_{H,L}$ calculated at the PBE0/cc-pVTZ-PP level of theory of stoichiometric $Cd_xSe_y^+$ species (with $x + y \leq 26$) on the averaged Cd-Se bond distance d(Cd-Se) and on the geometry motif. The diamond indicates the band gap value of bulk CdSe.

question of whether the intensity of the optical transitions of $Cd_xSe_y^+$ clusters can also be influenced by variation of the composition? To verify this, we calculate the normalized oscillator strengths f_{rel} as a measure of the overall absorption strength. Here, f_{rel} is the sum of the oscillator strengths up to the excitation energy of 5.0 eV normalized to the total number of electrons. Figure 4 shows f_{rel} in dependence of the number of Cd atoms x for different cluster sizes. From the course of the stoichiometric clusters (gray stars) with $x = y$, it can be deduced that the relative intensity is decreasing with each additional CdSe unit. It can be clearly seen that an increasing proportion of Cd leads to a greater overall intensity of the transitions. Interestingly, the relative transition strength of pure Se_y^+ clusters is almost zero for all species. Therefore the relative amount of Cd is the determining factor for high transition intensities which is also in accordance with experimental findings on CdSe NPs.[32]

Finally, it is investigated whether there is a relationship between geometric and optical properties? In order to exclude the influence of composition effects, only stoichiometric clusters are considered below. To quantify the cluster geometries by a number, the mean CdSe bond length d(Cd—Se) is calculated for all stoichiometric species. Again, all calculated optoelectronic properties (cf. Table S1) show a very similar behavior. Therefore, Figure 5 shows as an example the dependence of the HOMO-LUMO gap E_{HL} on d(Cd—Se) for stoichiometric species. There are several things that stand out. On the one hand, the mean bond length correlates with the type of the structural motif. For example, planar clusters have the smallest average bond lengths, 3d structures show larger values, and cage structures have even larger ones. Similar results were also found for neutral CdSe clusters.[33] A change in the structural motif causes a change in the number of neighboring atoms and therefore changes the coordination
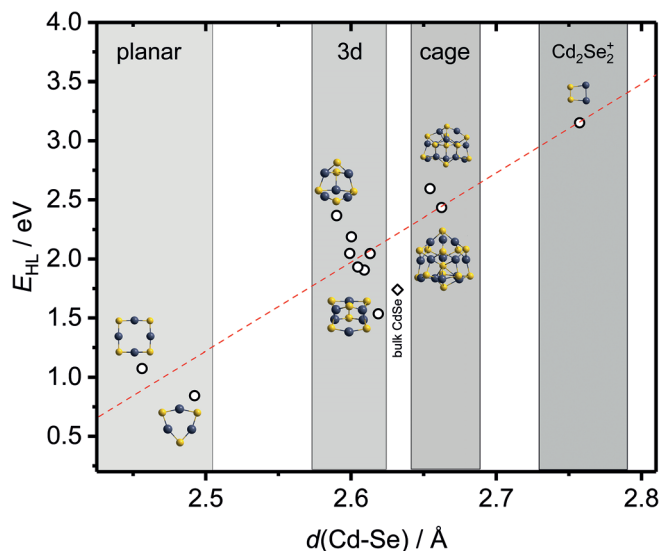
numbers. This directly affects the mean bond length. A linear regression (red line) highlights the correlation between d(Cd—Se) and E_{HL}. This also corresponds to a correlation between the geometry type and E_{HL}. For the cationic stoichiometric clusters, examined here, it holds, the larger d(Cd—Se), the larger E_{HL} is. Therefore, planar structures have the smallest and cage structures exhibit the largest E_{HL} value (with the exception of $Cd_2Se_2^+$). Again, this is a contrary size-dependent behavior as expected from larger CdSe QDs and also contrary to the HOMO-LUMO gap variation of neutral CdSe clusters. For latter it was found that E_{HL} increases from Cd_2Se_2 to Cd_4Se_4 which is followed by a decrease to Cd_5Se_5 and then only small changes are found up to $Cd_{12}Se_{12}$.[33] It should be emphasized that, in contrast to the cations, the structural motifs of the neutral clusters from Cd_5Se_5 to $Cd_{12}Se_{12}$ are 3d structures and no cage structure with a central atom is formed. Similar to Figure 3, here, the largest change in E_{HL} takes place at the transition from planar to 3d structures. As discussed before, the positive charge must be responsible for the unusual course of E_{HL}. In contrast to the neutral clusters, the extreme small E_{HL} values of $Cd_3Se_3^+$ and $Cd_4Se_4^+$ are as aforementioned caused by the split up of the degenerate HOMO orbitals (in case of the neutral clusters). This small splitting in the planar cations leads to this special behavior and thus, is mainly responsible for the increase of E_{HL} with d(Cd—Se). With the exception of $Cd_2Se_2^+$, a redshift of the HOMO-LUMO gap and optical gap with decreasing cluster size is generally observed. This redshift was also predicted for neutral $(CdS)_n$ clusters with $n = 2$–12 and was related to the formation of clusters with a lower effective dimensionality.[34]

4 | CONCLUSIONS

In this work, the compositional- and size-dependent variation of geometrical and optoelectronic properties of isolated $Cd_xSe_y^+$ clusters was extensively examined. New structural putative GM candidates were found. In case of Cd_x^+ clusters, linear chains are built up to $x = 5$. The structures of the mixed clusters strongly depend on the composition. A higher proportion of Cd leads to a preferred formation of planar structures. Larger stoichiometric clusters, like their neutral counterparts, are made up of alternating heteronuclear four-membered and six-membered heteronuclear bonded rings. Starting from a cluster size of 24 atoms, endohedral cage structures are formed with a Se atom at the center. All calculated optoelectronic properties: the HOMO-LUMO gap E_{HL}, the optical gap E_g and the first electronic excitation energy $E_{g,1}$ behave almost identical for different sizes and compositions. In general the average CdSe bond length d (CdSe) increases with the cluster size. Thus, there is a strong correlation between E_{HL} and the structural motif: E_{HL}(planar structures) < E_{HL}(3d Structures) < E_{HL} (cage structures). Mainly responsible for this increasing trend of E_{HL} with cluster size (or with the mean bond-length) are the small E_{HL} values of the planar structures $Cd_3Se_3^+$ and $Cd_4Se_4^+$. Optical properties strongly dependent on the stoichiometry and for a fixed number of atoms the values of EHL can be varied over a range of approximately 2 eV by changing the composition. In summary, it has been shown that cationic CdSe clusters differ fundamentally from the behavior of larger colloidal CdSe QDs, although, both are made up by the same structural subunits. However, in future studies it has to be examined to what extent the trends found here can be transferred to even larger isolated charged CdSe clusters.

DATA AVAILABILITY STATEMENT

The authors confirm that the data supporting the findings of this study are available within the article and its supplementary materials. All additional generated raw data are available from the corresponding author Marc Jäger on request.

ORCID

Marc Jäger https://orcid.org/0000-0001-5692-6900

REFERENCES

[1] Y. Shirasaki, G. J. Supran, M. G. Bawendi, V. Bulović, *Nat. Photonics* **2013**, *7*, 13 ISSN 17494885.

[2] Y. E. Panfil, M. Oded, U. Banin, *Angew. Chem. Int. Ed.* **2018**, *57*, 4274 ISSN 15213773.

[3] D. Bera, L. Qian, T. K. Tseng, P. H. Holloway, *Materials (Basel)* **2010**, *3*, 2260 ISSN 19961944.

[4] J. Klostranec, W. Chan, *Adv. Mater.* **2006**), ISSN 0935-9648, *18*, 1953. https://doi.org/10.1002/adma.200500786.

[5] J. M. Pietryga, Y. S. Park, J. Lim, A. F. Fidler, W. K. Bae, S. Brovelli, V. I. Klimov, *Chem. Rev.* **2016**, *116*, 10513 ISSN 15206890.

[6] M. Jäger, A. Shayeghi, V. Klippenstein, R. L. Johnston, R. Schäfer, *J. Chem. Phys.* **2018**, *149*, 244308 ISSN 0021-9606.

[7] M. Jäger, J. Schneider, R. Schäfer, *J. Phys. Chem. A* **2019**, *124*, 185.

[8] E. Sanville, A. Burnin, J. J. BelBruno, *J. Phys. Chem. A* **2006**, *110*, 2378 ISSN 10895639.

[9] C. B. Murray, D. J. Norris, M. G. Bawendi, *J. Am. Chem. Soc.* **1993**, *115*, 8706 ISSN 15205126, 93/1515-87.

[10] C. Leatherdale, W. Woo, *J. Phys. Chem. B* **2002**, *106*, 7619. https://doi.org/10.1021/jp025698c.

[11] D. Zhu, J. Hui, N. Rowell, Y. Liu, Q. Y. Chen, T. Steegemans, H. Fan, M. Zhang, K. Yu, *J. Phys. Chem. Lett.* **2018**, *9*, 2818 ISSN 1948-7185.

[12] H. Zhang, X. Peng, L. Sun, F. Liu, *MATEC Web Conf.* **2015**, *26*, 1006 ISSN 2261236X.

[13] V. Proshchenko, Y. Dahnovsky, *Phys. Chem. Chem. Phys.* **2014**, *16*, 7555 ISSN 1463-9084.

[14] A. Kasuya, R. Sivamohan, Y. A. Barnakov, I. M. Dmitruk, T. Nirasawa, V. R. Romanyuk, V. Kumar, S. V. Mamykin, K. Tohji, B. Jeyadevan, et al., *Nat. Mater.* **2004**, *3*, 99 ISSN 1476-1122.

[15] M. Troparevsky, L. Kronik, J. Chelikowsky, *Phys. Rev. B* **2001**, *65*, 033311 ISSN 0163-1829.

[16] M. C. Troparevsky, J. R. Chelikowsky, *J. Chem. Phys.* **2001**, *114*, 943 ISSN 00219606.

[17] P. Deglmann, R. Ahlrichs, K. Tsereteli, *J. Chem. Phys.* **2002**, *116*, 1585 ISSN 00219606.

[18] M. C. Troparevsky, L. Kronik, J. R. Chelikowsky, *J. Chem. Phys.* **2003**, *119*, 2284 ISSN 00219606.

[19] M. M. Sigalas, E. N. Koukaras, A. D. Zdetsis, *RSC Adv.* **2014**), ISSN 2046-2069, *4*, 14613 http://xlink.rsc.org/?DOI=c4ra00966e.

[20] M. Jäger, R. Schäfer, R. L. Johnston, *Nanoscale* **2019**, *11*, 9042 ISSN 20403372.

[21] M. Valiev, E. J. Bylaska, N. Govind, K. Kowalski, T. P. Straatsma, H. J. J. V. Dam, D. Wang, J. Nieplocha, E. Apra, T. L. Windus, et al., *Comput. Phys. Commun.* **2010**), ISSN 0010-4655, *181*, 1477. https://doi.org/10.1016/j.cpc.2010.04.018.

[22] C. Adamo, V. Barone, *J. Chem. Phys.* **1999**, *110*, 6158 ISSN 00219606, arXiv:1011.1669v3.

[23] K. A. Peterson, C. Puzzarini, *Theor. Chem. Acc.* **2005**, *114*, 283 ISSN 1432881X.

[24] D. Figgen, G. Rauhut, M. Dolg, H. Stoll, *Chem. Phys.* **2005**, *311*, 227 ISSN 03010104.

[25] A. D. Becke, *J. Chem. Phys.* **1993**, *98*, 5648 ISSN 00219606, z0024.

[26] K. A. Peterson, *J. Chem. Phys.* **2003**, *119*, 11099 ISSN 00219606.

[27] P. Álvarez-Zapatero, A. Aguado, *Phys. Chem. Chem. Phys.* **2019**, *21*, 12321 ISSN 14639076.

[28] B. C. Pan, J. G. Yan, J. Yang, S. Yang, *Phys. Rev. B – Condens. Matter Mater. Phys.* **2000**, *62*, 17026 ISSN 01631829.

[29] A. Alparone, *Theor. Chem. Acc.* **2012**, *131*, 1 ISSN 1432881X.

[30] L. G. Gutsev, N. S. Dalal, G. L. Gutsev, *J. Phys. Chem. C* **2015**, *119*, 6261 ISSN 1932-7447.

[31] K. A. Nguyen, P. N. Day, R. Pachter, *J. Phys. Chem. C* **2010**, *114*, 16197.

[32] J. Jasieniak, P. Mulvaney, *J. Am. Chem. Soc.* **2007**, *129*, 2841 ISSN 00027863.

[33] M. R. Farrow, Y. Chow, S. M. Woodley, *Phys. Chem. Chem. Phys.* **2014**, *16*, 21119 ISSN 14639076.

[34] G. L. Gutsev, R. H. O'Neal, K. G. Belay, C. A. Weatherford, *Chem. Phys.* **2010**), ISSN 03010104, *368*, 113. https://doi.org/10.1016/j.chemphys.2010.01.004.

SUPPORTING INFORMATION

Additional supporting information may be found online in the Supporting Information section at the end of this article.